1998

Geophysical Characterization, Redox Zonation, and Contaminant Distribution at a Groundwater/Surface Water Interface

John Lendvay
University of San Francisco, lendvay@usfca.edu

W A. Sauck

M L. McCormick

M J. Barcelona

D H. Kampbell

See next page for additional authors

Recommended Citation
Lendvay, J. M., W. A. Sauck, M. L. McCormick, M. J. Barcelona, D. H. Kampbell, J. T. Wilson, and P. Adriaens (1998), Geophysical characterization, redox zonation, and contaminant distribution at a groundwater/surface water interface, Water Resour. Res., 34(12), 3545–3559, doi:10.1029/98WR01736.

Authors
John Lendvay, W A. Sauck, M L. McCormick, M J. Barcelona, D H. Kampbell, J T. Wilson, and P Adriaens

WATER RESOURCES RESEARCH, VOL. 34, NO. 12, PAGES 3545–3559, DECEMBER 1998

Geophysical characterization, redox zonation, and contaminant distribution at a groundwater/surface water interface

J. M. Lendvay,[1] W. A. Sauck,[2] M. L. McCormick,[1] M. J. Barcelona,[1,3]
D. H. Kampbell,[4] J. T. Wilson,[4] and P. Adriaens[1]

Abstract. Three transects along a groundwater/surface water interface were characterized for spatial distributions of chlorinated aliphatic hydrocarbons and geochemical conditions to evaluate the natural bioremediation potential of this environmental system. Partly on the basis of ground penetrating radar measurements, a conductive sediment layer was detected from the shore out to at least 300 m offshore which exhibited gradients in redox pairs and contaminant profiles. The *cis*-Dichloroethene and 1-chloroethene were predominant in the presence of elevated methane and ferrous iron concentrations and depressed sulfate and aquifer solids-bound iron concentrations. The shallow monitoring points were generally hypoxic to aerobic and exhibited values of specific conductance reflective of near-shore lake water, indicating reoxygenation of the contaminant plume due to wave infiltration. The barge transect yielded trace contaminant concentrations and showed evidence of sulfate reduction. These analyses contributed to the understanding of processes affecting contaminant fate and transport at near-shore mixing zones.

1. Introduction

The St. Joseph, Michigan, National Priority List (NPL) site is located in southwestern Michigan along the eastern shore of Lake Michigan ~35 km north of the Indiana border (Figure 1, inset). The site has been contaminated with trichloroethene (TCE) by the discharge of industrial waste water into unlined lagoons and dry wells located ~750 m east of Lake Michigan between 1968–1976 [*Keck Consulting Services, Inc.*, 1986; *McCarty and Wilson*, 1992; *Wilson et al.*, 1994]. The practice of discharging the waste water to lagoons was continued until 1976 when the lagoons were drained and capped. In 1981 the unconfined aquifer under this industrial site was found to be contaminated with TCE, 1,2-dichloroethane, 1,1-dichloroethene (DCE), toluene, 1-chloroethene (vinyl chloride (VC), *cis*- and *trans*-1,2-DCE, ethene, and ethane. Further study of the aquifer contamination showed that two distinct plumes had formed as a result of a groundwater divide over which the suspected sources were situated [*Keck Consulting Services, Inc.*, 1986]. The western plume is bounded by Lake Michigan to the northwest, and the eastern plume is bounded by Hickory Creek to the east. This study focuses on the western plume at the interface with Lake Michigan.

The contaminated area is overlain by residential and agricultural use land with an approximate groundwater recharge rate of 55 cm yr^{-1} [*Tiedeman and Gorelick*, 1993]. Vegetation between the contaminant source and the lake is mostly grass and grapevines with some trees. The local topography is flat except for a 14 m vertical drop at the lake shoreline. The beachhead has an elevation slightly above that of the lake surface, and the water table is located from 0 to 2 m below ground surface. Shoreline elevation is affected by wave erosion and seiche effects of the lake varying ~1 m either way on a seasonal basis. Additionally, the beach is littered with concrete slabs from previous attempts to deter erosion as well as large pieces of embedded driftwood. The geology of the site is primarily medium to fine sand with some silt having been formed by eolian and lacustrine modification of glacial deposits. The upper unconfined layer is underlain by a lacustrine clay that is believed to be hydraulically impermeable [*McCarty and Wilson*, 1992; *Kitanidis et al.*, 1993; *Semprini et al.*, 1995].

The chlorinated solvents (predominantly TCE) were reported previously on the basis of groundwater analyses of five up-gradient transects (Figure 1) along the western segment of the plume [*McCarty and Wilson*, 1992; *Kitanidis et al.*, 1993] to have undergone extensive dechlorination to *cis*-, *trans*-, and 1,1-DCE, VC, ethene, and ethane. Considering spatial chemical distributions, it was estimated that 20% of the TCE had dechlorinated to ethene, predominantly under sulfate-reducing and methanogenic conditions [*Semprini et al.*, 1995]. On the basis of a regional groundwater flow model, fluxes of all organic compounds into Lake Michigan were estimated to be of the order of 8.4–17 kg yr^{-1} [*Tiedeman and Gorelick*, 1993; *Wilson et al.*, 1994]. The production of VC, a known carcinogen, during reductive dechlorination and the recreational use of the area north of the site motivated the current study of natural plume-controlling processes at the groundwater/surface water interface (GSI).

2. Background

2.1. Groundwater/Surface Water Interfaces

Whereas inland GSIs are generally characterized by a relatively sharp front between the two water bodies, this feature is less distinctive for coastal regions experiencing seiche action

[1]Environmental and Water Resources Engineering, Department of Civil and Environmental Engineering, University of Michigan, Ann Arbor.
[2]Department of Geology, Institute for Water Sciences, Western Michigan University, Kalamazoo.
[3]Also at IST Building, Ann Arbor, Michigan.
[4]Subsurface Protection and Remediation Division, U.S. Environmental Protection Agency, Ada, Oklahoma.

Paper number 98WR01736.
0043-1397/98/98WR-01736$09.00

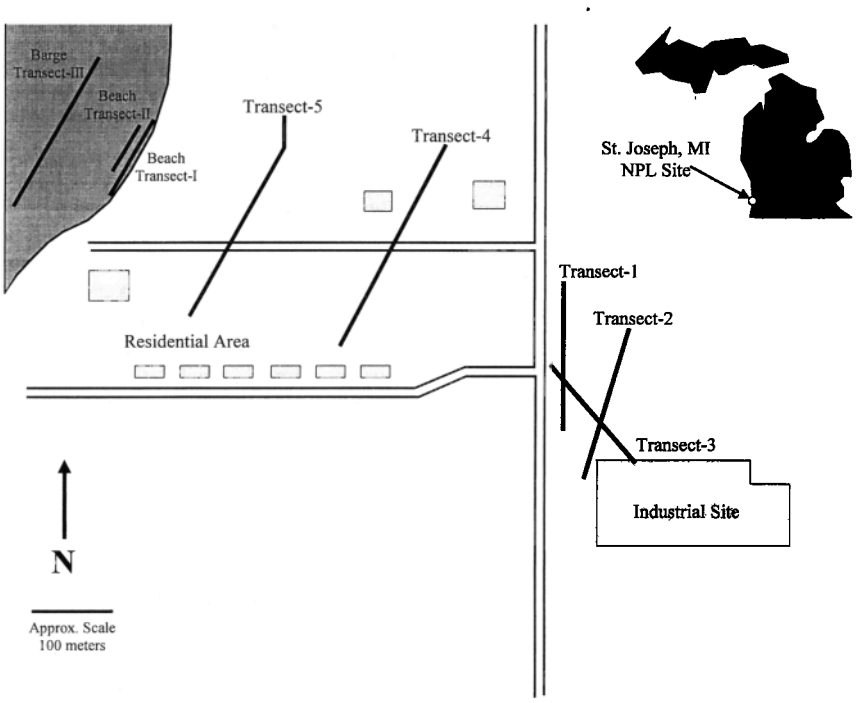

Figure 1. Geographical location (inset) and plan view of historical transects at the St. Joseph, Michigan, superfund site.

and beach erosion/accretion [*Lee*, 1977; *Cherkauer and McBride*, 1988]. In the latter regions the term groundwater/surface water mixing zones might be more appropriate. These zones are extremely dynamic hydrologically, characterized by wave run-up and infiltration, groundwater seepage into and out of the surface water body, groundwater/surface water mixing, and possible ebullition processes as a result of gases produced from anaerobic microbial activity. Moreover, the spatial distribution of the depositional system of the surface water sediments greatly affects groundwater (and contaminant) flow [*McBride and Pfannkuch*, 1975; *Cherkauer and Nader*, 1989]. For example, the Lake Michigan shoreline exhibits different depositional facies in fairly close proximity to one another, ranging from shore-parallel alignment to various fluvial cut-and-fill channel structures associated with the filling of ancestral river valleys (e.g., St. Joseph River, Benton Harbor) (W. A. Sauck, personal communication, 1994). In the latter the channel directions would be expected to greatly control groundwater and contaminant flow.

The relative positions of the water table under a beach and the mean shoreline topography influence beach accretion and erosion by affecting the amount of water that infiltrates into the beach rather than returning as backwash [*Duncan*, 1964]. Thus the location of groundwater seepage (point of contaminant emergence) cannot be predicted on the basis of hydraulic head differences alone as it is affected by "pumping effects" due to wave run-up and infiltration and the stratification of zones with different hydraulic conductivities as the result of sediment deposition. Moreover, heterogeneities in the thickness of the sediment layer separating the aquifer from surface water bodies affect the distance of offshore seepage [*Cherkauer and Nader*, 1989]. The hydrodynamic effects of a GSI on a contaminant plume have been extensively described [*Sacks et al.*, 1992; *Shedlock et al.*, 1993; *Vanek*, 1993; *Devito et al.*, 1996]. However, the effects of this physical interaction on the aquifer oxidation-reduction capacities and in situ microbial activity has received limited attention [*Strobel*, 1995].

2.2. Redox Zonation in Aquifers

An adequate understanding of the distribution of in situ redox processes is central to the interpretation and prediction of the fate of contaminants in environmental systems. Contaminated aquifers exhibit spatial and temporal changes in redox chemistry as the result of microbial respiratory processes and recharge from precipitation events on a seasonal basis. The presence of microbial carbon and energy sources, such as fuel hydrocarbons and natural organic matter (TOC), will result in a gradual depletion of available electron acceptors and in anaerobiosis depending on how well the system is poised. The resistance of aquifer environments to becoming reduced can be represented by their oxidation capacity (OXC), which includes the dissolved and aquifer solid-associated concentrations of potential electron acceptors as well as the electron-accepting capacity of each species [*Barcelona and Holm*, 1991]. It should be noted that the OXC based on dissolved constituent analysis alone has been found to underestimate the true redox buffer capacity of an aquifer, as Fe^{3+}, Mn^{4+}, and organic carbon are mainly associated with the aquifer mineral phase. On the basis of studies at two uncontaminated sandy aquifers it has been estimated that only up to 2% of OXC can be captured in the aqueous phase [*Barcelona and Holm*, 1991]. This is particularly relevant to aquifers where ferric iron- and sulfate-reducing processes are dominant and reduced species rapidly precipitate as iron sulfides or iron hydroxides [*Heron and Christensen*, 1995; *Christensen et al.*, 1994].

Microbial anaerobic degradation and kinetics of organic matter (anthropogenic or natural) oxidation are inherently nonequilibrium systems because these processes tend to occur in chains of reactions starting with fermentation. *Postma and Jakobsen* [1996] recently proposed a partial equilibrium ap-

proach to describe this succession of redox zonation. This approach is based on the rationale that since fermentative byproducts such as acetate and hydrogen are typically observed at orders of magnitude lower concentrations than terminal electron acceptor consumption [*Chapelle et al.*, 1996; *Lovley and Chapelle*, 1995; *Lovley and Goodwin*, 1988] the fermentative step must be rate-limiting (or the terminal electron-accepting processes (TEAPs) approach chemical equilibrium), and the kinetics of the overall reaction cannot be described from energy yield of the TEAP alone. Cooccurrence of iron and sulfate reduction, as well as methanogenesis, in aquifers and lake sediments cannot be predicted on the basis of thermodynamic considerations [*Wersin et al.*, 1991; *Simpkins and Parkin*, 1993]. Using the partial equilibrium approach, simultaneous iron and sulfate reduction were explained by iron oxide stability, *p*H of the pore water, and sulfate concentration. It was found that more distinct redox zonation would be expected in sediments with a confined stability range of iron oxides.

In addition to horizontal TEAP stratification along the path of groundwater flow a previous study of this site provided evidence of vertical stratification of TEAPs and contaminant distribution [*Semprini et al.*, 1995]. Specifically, this study showed that sulfate-reducing processes were dominant in shallow zones of the plume corresponding to an accumulation of *cis*-DCE as the dominant contaminant dechlorination product. Methanogenesis was the dominant TEAP in deeper zones, with VC and ethene present as the main dechlorination products. On the basis of predictions from a modified modular three-dimensional finite-difference groundwater flow model (MOD-FLOW) model developed for this site [*Tiedeman and Gorelick*, 1993], the authors hypothesized that recharge-dominated groundwater flow was the reason for this vertical stratification. Thus the contaminants and any organic driving force originating from the source would be expected to migrate deeper into the aquifer, resulting in more reduced conditions (e.g., methanogenesis) and more extensively dechlorinated products (e.g., VC and ethene) in deeper zones.

2.3. Effect of Redox Conditions on Chlorinated Aliphatic Hydrocarbons Transformation

Documented field characterizations of contaminant and product distribution in anaerobic contaminated aquifers have indicated that TCE undergoes variable degrees of natural dechlorination (reviewed by *Rifai et al.* [1995]). It is not clear which environmental characteristics determine the extent of dechlorination or which organisms are the causative agents. However, certain correlations between product distribution and dominant TEAPs have been observed. Under anaerobic conditions conducive to methanogenesis or sulfate reduction, TCE was shown to be either completely dechlorinated to ethene or to DCE, respectively [*Bagley and Gossett*, 1990; *Pavlostathis and Zhuang*, 1991, 1993; *Haston et al.*, 1994; *Semprini et al.*, 1995]. On the contrary, aerobic conditions have been shown to support cometabolic (cooxidation) reactions in the presence of specific enzyme-inducing substrates (reviewed by *Wackett* [1995]). Hypoxic environments where iron-reducing and denitrifying conditions prevailed were shown to sustain either anaerobic mineralization [*Bradley and Chapelle*, 1996] or dechlorination [*Adriaens et al.*, 1997; M. L. McCormick and P. Adriaens, Reductive dechlorination of tetrachloroethene under iron reducing conditions, submitted to *Journal of Environmental Quality*, 1998] processes.

Halorespiration (energetic coupling of dechlorination reactions to growth) of tetrachloroethene (PCE), TCE, and DCE under reduced conditions represents one of the few growth-based processes affecting the fate of this class of contaminants (reviewed by *Holliger and Schumacher* [1994]). Additionally, anaerobic reductive dechlorination may be catalyzed abiotically in the presence of reduced metal sulfide minerals [*Kriegman-King and Reinhard*, 1992; *McCormick et al.*, 1998] or by humic acid-mediated redox reactions [e.g., *Curtis and Reinhard*, 1994]. The former may be of importance in aquifers where significant iron or sulfate reduction takes place. The goals of this study are (1) to determine the applicability of ground-penetrating radar (GPR) and sonar to guide sampling programs, (2) to evaluate the effects of GSIs on the TEAPs and contaminant distribution, and (3) to determine the most likely microbial processes affecting intrinsic remediation of the contaminants at the GSI.

3. Materials and Methods

3.1. Field Sampling

The 2 year GSI field sampling program was coordinated between the University of Michigan (UM, Ann Arbor, Michigan), the U.S. Environmental Protection Agency (EPA) Region 5 (Chicago, Illinois), the U.S. EPA Subsurface Protection and Remediation Division (Ada, Oklahoma), the Institute for Water Sciences at Western Michigan University (Kalamazoo, Michigan), and Allied Signal Corporation (now Bosch Braking Systems, St. Joseph, Michigan). The GSI sampling plan consisted of 14 borings along three transects (Figure 2); 10 borings were performed on the beachhead (denoted 55-AA through 55-AJ), and 4 borings were performed ~100 m offshore (denoted barge-1 through barge-4). Real-time gas chromatographic and ion chromatographic analyses were performed to help guide the selection of additional borings as well as elevations of sample collection.

Five shore-perpendicular (0–122 m SW at 30.5 m intervals) and three shore-parallel (50, 100, and 300 m NW, relative to wood pilings) lines of Lake Michigan bottom sonar and GPR measurements were performed to help in the selection of offshore sampling locations (Figure 2). Sonar and GPR measurements used a bottom-towed polyvinyl chloride (PVC) radar sled equipped with a downward looking 145 MHz dipolar antenna coupled to a SIR-10 ground-penetrating radar system (Geophysical Survey Systems, Inc. (GSSI), North Salem, New Hampshire) and an upward looking sonar transducer. The sonar system used was a Lowrance X-16 with the sled-mounted transducer model HS-WA transmitting at 192 kHz. Along-line marks were inserted into the sonar record at 50 m intervals, coincident with the GPR fiducial marks. The analog records were later digitized for construction of the bathymetric map.

The dipolar GPR antenna element was positioned ~6 cm above the lake bottom and was oriented with its long axis in the direction of the traverse line. The single antenna used with this impulse radar system was driven by a GSSI model 769DA transceiver card, and the return signal was digitized at 512 points with 16-bit precision during the 240 ns scan length. A constant gain function was used along the entire profile. The pulse repetition rate was 50 kHz, easily producing radar depth scans at horizontal intervals of about a centimeter at reasonable towing velocities.

This approach allowed collection of concurrent subbottom and water depth information at the same point, eliminating

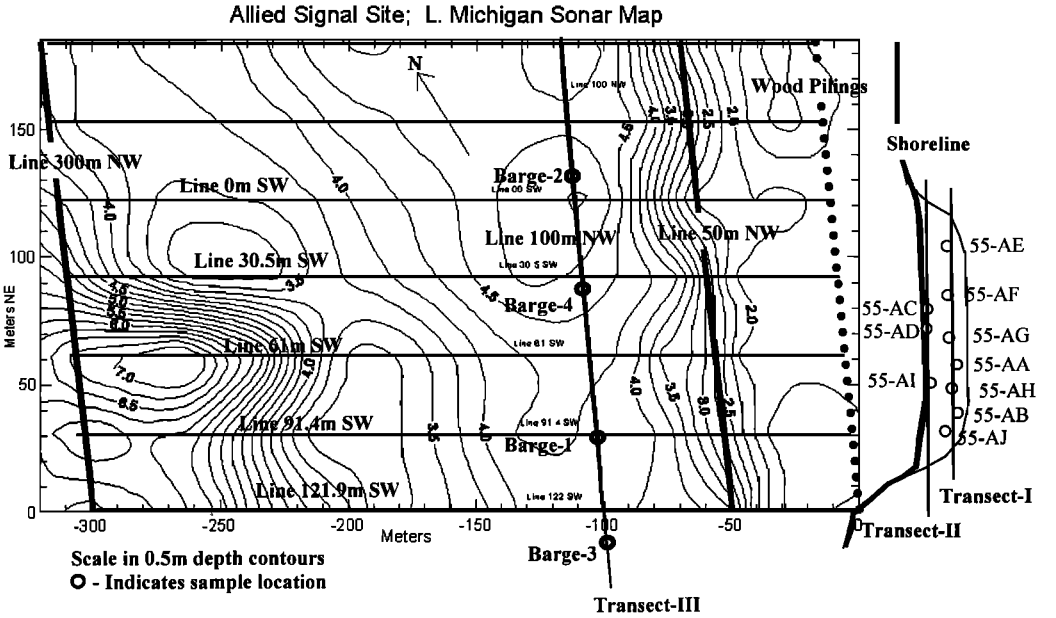

Figure 2. Survey map of ground-penetrating radar (GPR) and SONAR profiling, indicating beach and barge transects overlain on SONAR depth contour map of Lake Michigan bottom. Depth contours are in meters below lake surface.

problems of rectifying boat-gathered sonar with sled-gathered GPR data (at a slant distance of 30 m from the boat). Horizontal and vertical scales of the GPR profiles were rectified so that scales in the water and in the subbottom were identical. GPR measurements are based on the interpretation of reflection patterns resulting from the interaction of intense short electromagnetic pulses with features of the subsurface [*Daniels*, 1989]. Thus GPR pattern interpretation was governed by media electromagnetic properties such as conductivity σ, relative permittivity ε_r, and relative magnetic permeability μ_r and has been applied to the characterization of lake sediments [*Daniels*, 1989; *Delaney et al.*, 1992; *Campbell et al.*, 1997] and delineation of groundwater contamination [*Daniels*, 1989; *Benson*, 1992; *Lawton et al.*, 1994; *Sauck et al.*, 1997; *Nash et al.*, 1997]. The acquisition of GPR profiles using a submerged bottom-towed antenna in the current study was experimental and has only been reported on recently [*Campbell et al.*, 1997].

Groundwater and aquifer solid samples were collected by installing temporary sample points using steel geoprobe rods (2.5 cm diameter) with a slotted screen point assembly. The sample point consisted of a 61 cm long slotted screen with fifteen 0.5 mm wide by 51 mm long slots. Since the beachhead was inaccessible to a truck-mounted geoprobe the rods and sampling points were installed either manually with a fence post driver or with the help of a generator-powered 80 lb electric hammer. Offshore samples were obtained using a geoprobe truck mounted onto a barge and anchored in place with the aid of a tugboat and large steel pylons or anchors [*Barcelona*, 1994]. During the offshore sampling process the geoprobe rods were restricted from bowing in the lake by a shroud of 0.64 cm thick PVC pipe (10 cm diameter) attached to a steel plate (2.5 cm thick) that encircled and provided lateral support to the geoprobe rods. This assembly allowed for sampling in waves of up to 70 cm. After inserting the screen and rods to the desired depth the sample point was purged and sampled using a peristaltic pump. In all cases the piezometric surface was <3 m below the peristaltic pump, which is well within the pump's differential head requirements. Successive samples were collected across the contaminated aquifer thickness at ~1 m depth increments down to 5–10 m below the piezometric surface.

At each sample elevation, *p*H, dissolved oxygen, chlorinated aliphatic hydrocarbons (CAHs), volatile organic carbons (VOCs), nitrate, sulfate, chloride, specific conductance, reduction potential, dissolved iron, and sulfide were analyzed. The standard sampling protocol was first to measure the hydraulic conductivity using a drawdown test before developing the sample point. The sample point was then developed, and suspended solids were collected in glass sample jars using a peristaltic pump. Aquifer solids were saturated with groundwater and sealed without headspace and immediately stored on ice until delivery to the UM laboratories where samples were stored at 4°C until used. After developing each sample location the groundwater was pumped until consistent dissolved oxygen readings were obtained. Readings were considered consistent when dissolved oxygen changed <0.2 mg L^{-1} over 5 min. Dissolved oxygen, *p*H, and temperature were recorded continuously during this stage. Once the field readings stabilized, water samples were collected for on-site analysis using a mobile laboratory or preserved for later analyses.

3.2. Groundwater and Aquifer Solid Analyses

Samples for VOC analyses and aqueous inorganic analyses were collected and immediately preserved and placed on ice for delivery to EPA laboratories for analysis. VOCs were analyzed using purge and trap with gas chromatography for chlorinated ethenes and aromatic hydrocarbons [*American Public Health Association*, 1992] and headspace gas chromatography described by *Kampbell et al.* [1989] for methane, ethene, and ethane. Total Organic Carbon (TOC) was analyzed using EPA method 9060 [*U.S. Environmental Protection Agency* (*EPA*),

1986]. Inorganic analyses (nitrate and nitrite nitrogen, sulfate, and aqueous iron) were performed using EPA method 353.1 or Waters Capillary Electrophoresis method N-601. Sulfur containing anions including sulfate, thiosulfate, sulfide and sulfite were analyzed for sample locations 55-AE through 55-AJ using a Waters 640 capillary electrophoresis unit.

Chloride was analyzed utilizing EPA standard method 325.3 [*EPA*, 1979]. Dissolved oxygen, temperature, *p*H, specific conductance, and oxidation-reduction potential were determined at the sample location immediately upon extraction of the groundwater from the sample point. Dissolved oxygen was analyzed using an Orion Model 840 dissolved oxygen meter. Temperature, *p*H, and specific conductance were analyzed using an Orion Model 250A meter with a combination probe. Oxidation reduction potential was determined using a redox probe in accordance with standard method 2580B [*American Public Health Association*, 1995]. Additionally, beach groundwater samples 55-AE through 55-AJ (August 1995) were analyzed for TOC, some aromatic hydrocarbons (benzene, toluene, ethylbenzene, and xylenes), sulfur oxyanions (sulfite and thiosulfate), and sulfide. Finally, solid samples collected from beach samples 55-AE through 55-AJ were analyzed for acid extractable iron (II) and iron (III) solids.

Aquifer solid samples obtained from locations 55-AE through 55-AJ were extracted in deoxygenated hydrochloric acid, and iron (II) was determined using a colorimetric procedure modified from *Lovley and Phillips* [1987] and *Heron et al.* [1994]. This procedure consists of a 0.5 M HCl acid extraction for 1 hour to measure a combination of most of the Fe^{2+}, amorphous-FeS, some siderite ($FeCO_3$), and traces of pyrite (FeS_2) and magnetite (Fe_3O_4) [*Heron et al.*, 1994]. Bioavailable ferric iron (as previously defined by *Lovley and Phillips* [1987]) was measured using the same procedure but with the filtered extract being reduced by 0.25 M hydroxylamine to Fe^{2+} prior to color formation. Iron (III) was then determined by difference. Dissolved iron (II) was quantified using FerroZine (3-(2-pyridyl)-5,6-bis(4-phenylsulfonic acid)-1,2,4-triazine, monosodium salt, monohydrate) in a tris(hydroxymethyl)-aminomethane buffer solution at *p*H 8.0 [*Stookey*, 1970; *Gibbs*, 1976]. The analysis was performed at 562 nm on a Varian Carry 3 UV-vis spectrophotometer, and iron (II) was quantified using a five-point external standard curve.

4. Results and Discussion

4.1. Geophysical Characterization

Offshore GPR and sonar data proved to be essential in guiding the sampling program for the interpretation of the offshore boring profiles with respect to contaminant transport and to be helpful in predicting the zone of interaction of the plume with the lake water. The shore parallel profile (exemplified for 100 m NW, Plate 1a) showed a strong, continuous upper radar reflector A (0–2 m below lake bottom) which is present regionally from Benton Harbor, Michigan, to Burns Harbor, Indiana (W. A. Sauck, personal communication, 1994). Overall, the remarkable continuity of reflectors A-C (some of which are traceable for the full 500+ m of line length) and the uniformity in the shore-parallel plane strongly imply shore-parallel alignment of deposition of these lacustrine sediments (e.g., reflectors B and C below the strong upper reflector). Moreover, the absence of fluvial cut-and-fill channel structures would preclude the existence of preferential groundwater flow channels into the lake.

Where sands are present above and below reflector A (Plates 1a and 1b), as at this site, the cause of the reflection may be two phenomena: (1) a porosity/sorting change resulting in differences in water content ε_r or (2) an abrupt change in electrical conductivity σ. The former case implies transition to at least thin layers of coarser sands and gravels or to silts and clays, neither of which were reported at this level during subsequent subsurface sampling. However, in otherwise uniform sands, reflections can be produced by a very thin lamina of clay or silt, which might have been missed at the sampling sites. Thus the upper GPR reflector is most likely a physical or stratigraphic boundary since permittivity normally dominates over conductivity in the reflection coefficient. That would constitute a porosity or permeability boundary, which may in turn provide a downward barrier to circulation of oxygenated lake waters that could ultimately result in a difference in aqueous chemistry. The second phenomenon might be due to low-conductivity lake water in the sands above and higher-conductivity groundwater (or stagnant lake water) below that boundary. In the latter case the boundary would be due to higher dissolved ion concentrations below as a result of the long residence time of the groundwater or connate lake water and should be apparent as a significant boundary for other chemical constituents besides the ionic constituents that contribute to electrical conductivity. The effect of the elevated conductivity on the GPR records would be in muting or attenuating reflections from all underlying stratigraphic reflectors.

The elevation versus specific conductance profiles from the beach and barge sampling points (Figure 3) directly support the argument that GPR profiles correlate to more conductive groundwater, indicating the region of contamination on the basis of the following rationale. First, all profiles showed a clear delineation of shallow zones with specific conductance values between 200 and 500 μS cm^{-1}, similar to that of the surface water, and deeper zones with elevated specific conductance >550 μS cm^{-1} (Figure 3a). In each transect this high-conductance layer was underlain by another zone of lower specific conductance. Second, in all transects the specific conductance was significantly correlated ($\rho \geq 0.90$ and $\alpha = 0.01$) to elevated chloride concentrations presumably resulting from reductive dechlorination reactions (Figure 3b). In the barge transect (transect III) a significant negative correlation ($\rho = -0.91$ and $\alpha = 0.01$) was obtained with sulfate; that is, the highest sulfate concentrations were in zones with the lowest specific conductance (Figure 3c). This observation will be further discussed in the context of redox zone delineation. Third, the elevated specific conductance layer was characterized by the presence of contaminants in all transects (see contaminant distribution and potential for intrinsic bioremediation section).

The shore-perpendicular profiles (exemplified for 30.5 m SW, Plate 1b) showed the regional marker reflector A at 0.5–3 m depth below lake bottom and an interfering top-of-water reflector in shallow near-shore waters. At all locations in previous Lake Michigan work the upper reflection is clearly an age boundary; that is, a geologic nonconformity separating modern, mobile, oxygenated sands from Pleistocene sands and silts (this location), Pleistocene clays and tills (between this site and St. Joseph, Michigan), and Mississippian shales (16 km SW of this site). The layered sands and silts below the nonconformity were clearly visible between 50 and 150 m offshore from the row of wooden pilings. At lines 91.4 m SW and 121.9 m SW these layers (at the target depth range of 5–8 m) sloped or dipped shoreward. At line 61 m SW these layers had an un-

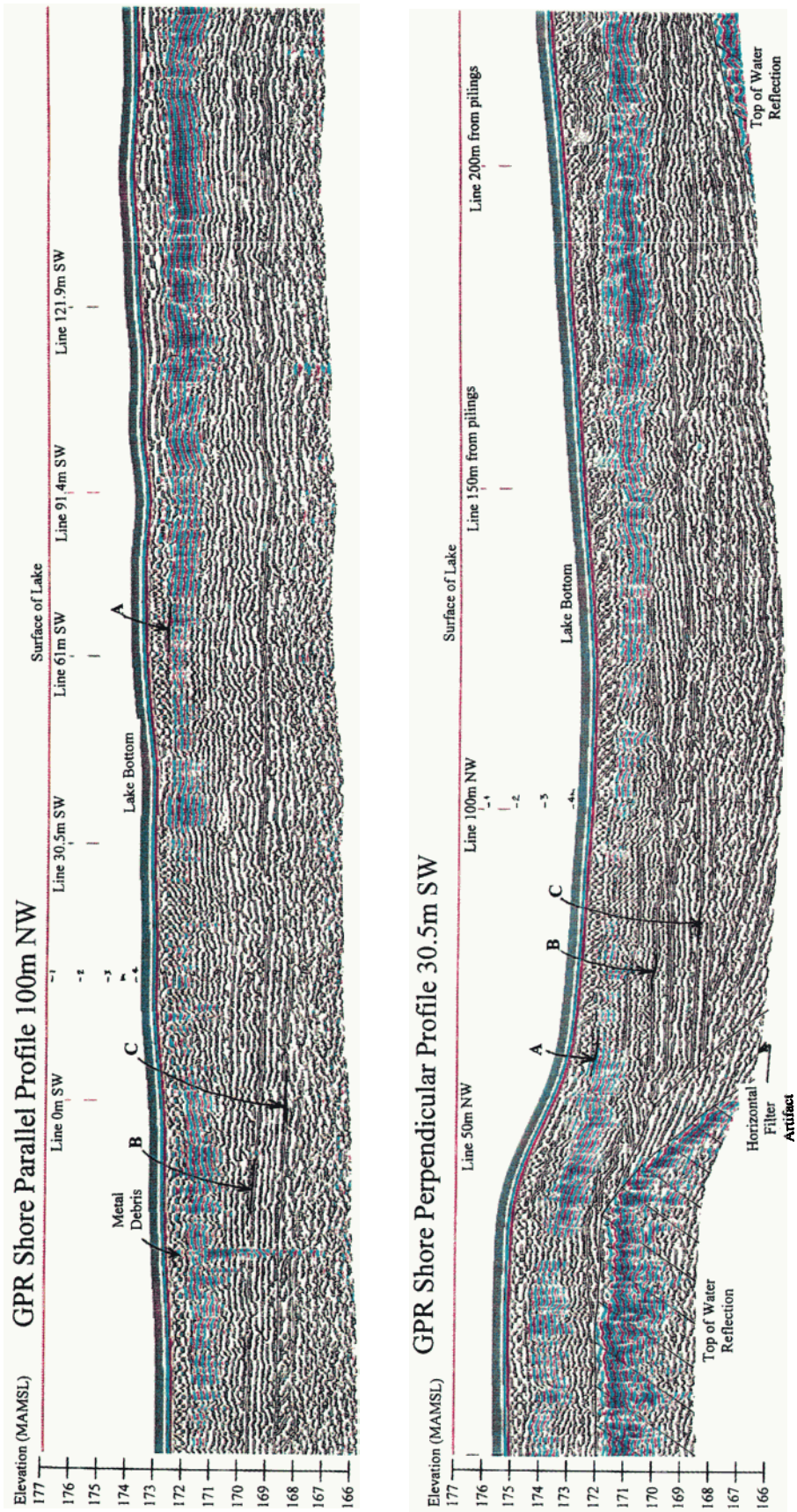

Plate 1. Segments (a) of shore-parallel GPR profile 100 m NW and (b) of shore-perpendicular GPR profile 30.5 m SW. All distances are relative to wooden pilings. Reflector A corresponds to a zone of high specific conductance (Figure 3) and is reflecting either (1) a porosity/sorting change resulting in differences in water content or (2) an abrupt change in electrical conductivity. Reflectors B and C reflect depositional facies of lacustrine sediments.

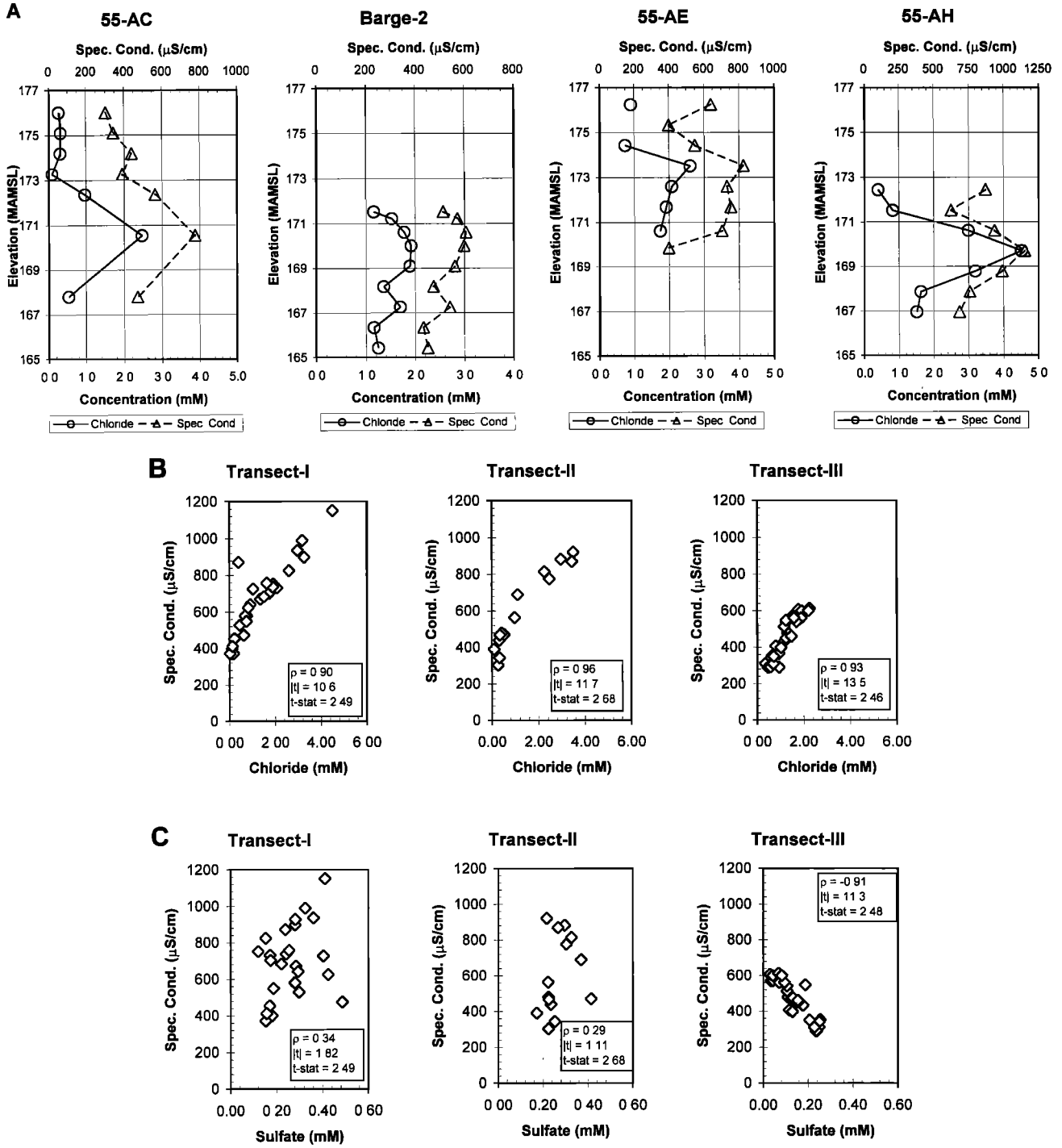

Figure 3. (a) Well-specific conductance and chloride elevation profiles, (b) specific conductance and chloride scattergrams, and (c) specific conductance and sulfate scattergrams at transects I–III. Statistical analyses shown consist of correlation coefficient ρ, $|t|$ based on a two-tailed t test, and the statistical determination of t (t-stat) using $\alpha = 0.01$ (99% confidence interval).

dulating nature and locally dipped lakeward. Lines 0 and 30.5 m SW show approximately horizontal strata (reflectors B and C) underlain by a deeper broad, gentle depression. These variable stratigraphic dips have implications for local groundwater (and plume) flow direction. Whereas shoreward dips could influence plume emergence nearer to shore, horizontal or lakeward dips would result in offshore emergence. The bathymetric contour map (Figure 2) indicates the existence of a trough (5 m deep) at ~100 m offshore, which was the predicted locale of emergence of the plume. This trough was chosen for transect III.

The application of GPR to the direct detection and delineation of groundwater contamination is fairly recent and has been successful particularly in identifying both light and dense nonaqueous phase liquids (NAPLs) [*Olhoeft et al.*, 1988; *Maxwell and Schmock*, 1995; *Sauck et al.*, 1997; *Bermejo et al.*,

1997]. The detection sensitivity is due in part to the different electrical properties of these phases as compared to background waters. The dissolved phase of a hydrocarbon plume cannot be detected directly because of the generally low concentrations and lack of charge carriers (hydrocarbons are electrically neutral). However, indirect geophysical evidence can be obtained on the basis of wave attenuation of the GPR signals due to increased specific conductance because of the dissolution of ions (bicarbonate, sulfate, nitrate, iron, manganese, silica, and others) from aquifer solids after reaction with the organic or carbonic acids resulting from hydrocarbon degradation [*King and Olhoeft*, 1989; *Sauck and McNeil*, 1994; *Monier-Williams*, 1995; *Sauck et al.*, 1997].

Attenuation visible on the GPR profiles in the current study suggested a zone of higher bulk electrical conductivity from the shore out to the predicted point of emergence, which was associated with elevated chloride, iron, sulfate (beach transects), and contaminant concentrations in groundwater samples. Analysis of up-gradient transects indicated a decrease in TOC from the presumed source toward the shore, hypothesized to be due to methanogenesis and cometabolic reductive dechlorination processes [*McCarty and Wilson*, 1992]. The TOC was shown to be composed of low molecular weight aromatic (e.g., benzoic and methylbenzoic) and aliphatic (e.g., pentanoic and hexanoic) acids, which may have resulted from the microbial metabolism of either natural organic matter [*McMahon and Chapelle*, 1991] or fuel hydrocarbons (e.g., xylenes and benzene) associated with the spill [*Cozzarelli et al.*, 1994].

4.2. Redox Zone Delineation

The interpretation of oxidation-reduction conditions of the three transects along the GSI was based on the spatial distribution of redox-active species (Figures 4b and 4c and Table 1) and silver electrode redox measurements (Figure 4d).

4.2.1. Transect I (55-AE to 55-AJ). The redox plot (Figure 4d) indicates the existence of a reduced (−23 to −60 mV) zone in the NE section of the transect at elevations from 173 to 170 m above mean sea level (MAMSL), which was surrounded by a more oxidized (123–200 mV) zone. The reduced zone corresponded to elevated methane concentrations and depletion of oxygen and nitrate and/or lower concentrations of sulfate, relative to the oxygenated zone. The elevation plot of sample points 55-AH (SW) and 55-AE (NE) indicated a reduction of the groundwater in the NE direction. The shallow sampling points (174–176 MAMSL in 55-AE and 172.5 MAMSL in 55-AH) contained appreciable concentrations of oxygen (0.06–0.25 mM), while the deeper sampling points reveal either decreased sulfate (55-AH) or elevated methane (55-AE) concentrations.

Nitrate and nitrite were not quantified separately during analyses because previous studies suggested that nitrate-reducing processes were minor compared to the more reduced microbial processes in the up-gradient section of the contaminant plume [*Semprini et al.*, 1995]. Therefore it was difficult to assess the significance of denitrification at the site. Total concentrations of nitrogen-containing aqueous species did not exceed 0.12 mmol and were usually below 0.05 mmol (Figure 4b). Dissolved and aquifer solid-associated analyses were performed to evaluate the distribution of iron species along transects I and II. Elevation profiles of dissolved Fe (II), acid extractable Fe (II) solids [*Heron et al.*, 1994], and bioavailable iron (III) solids [*Lovley and Phillips*, 1987] are shown for sample points 55-AE to 55-AI (Figure 4b and Table 1 for aqueous iron (II) and Figure 5 and Table 1 for aquifer solids-bound iron).

On the basis of these data, several trends may be observed. Dissolved iron (II) concentrations were extremely low (≤0.5 mg L^{-1}, Table 1; ≤0.01 mmol, Figure 4b) when compared to more typical groundwater values in Michigan [*Chapelle et al.*, 1996] and did not resolve differences in past or present iron reduction with depth or location. This observation is most likely due to the precipitation of Fe^{2+} as mixed valence iron oxides (e.g., magnetite) or iron sulfides (e.g., amorphous FeS and mackinawite) [*Heron et al.*, 1994]. However, aquifer solid extraction clearly showed a 50%–90% reduction in bioavailable iron (III) with depth, relative to the shallow sampling points (Table 1 and Figure 5a). This decrease coincided with the most highly contaminated sampling elevations and a predominance of *cis/trans*-DCE or TCE (167–170 MAMSL at 55-AH). A second notable trend was a general decrease in bioavailable iron (III) in the NE direction or from the fringes to the apparent central flow line of the plume (55-AH to 55-AE). Bioavailable iron (III) concentrations at comparable elevations (e.g., 170 MAMSL) decreased from 158 to 5 mg kg^{-1} aquifer solids (Table 1 and Figure 5a). On the basis of extensive solids extraction (21 days; 5 M HCl acid) performed on samples from sample points 55-AB and 55-AD the bioavailable iron levels represented ~1%–6% of total extractable iron [*Lendvay et al.*, 1995]. In addition to the decrease in bioavailable iron (III) at 170 MAMSL in the NE direction, extractable iron (II) concentrations increased from 220 (55-AH) to 698 mg kg^{-1} aquifer solids (55-AE, see Table 1 and Figure 5b).

4.2.2. Transect II (55-AC to 55-AI). This transect, which was closest to the lake shore, showed positive redox potentials, except for one sampling point at 170.5 MAMSL in sample point 55-AC. Overall, the values were 50–80 mV higher than those in transect I (Figure 4d). The high redox potentials at shallow depths coincided with elevated oxygen concentrations (>0.06 mmol or >2.0 mg L^{-1}) and low specific conductance reflective of lake water (250–420 μS cm^{-1}, Figure 3a). This observation supports the phenomenon of wave run-up and lake water infiltration affecting the top 3 m of the plume. Additionally, methane concentrations were 1 order of magnitude lower, and sulfate concentrations were 1.5 times higher, than in transect I (Figure 4c). The bioavailable iron concentrations of the aquifer material of sample point 55-AI (Table 1) were similar to those obtained for sample points near the center of transect I (55-AC and 55-AF), indicating possible current or past iron reduction.

4.2.3. Transect III (B2 to B3). Of all transects the lake bottom subsurface was clearly the most reduced, with measured redox values ranging from 160 to −145 mV. The magnitude of the negative redox values depended on the barge location, but reduced zones were generally confined to an elevation of 172–169 MAMSL (Figure 4d). The most SW located boring, barge 3, did not show any negative readings (data not shown) and, on the basis of the general flow path of the contaminant plume and lack of detectable contaminant concentrations, was located outside the contaminated area. The reduced region at the other barge locations coincided with depleted sulfate concentrations (e.g., barge 2, Figures 4c and 4d) and slightly elevated (0.01–0.08 mmol) methane concentrations. Oxygen concentrations in the most shallow sampling points did not exceed 0.06 mmol or ~2 mg L^{-1} and ranged from 0 to 0.04 mmol in the reduced zone. In this case some of the measured redox values (e.g., −145 mV) were sufficiently

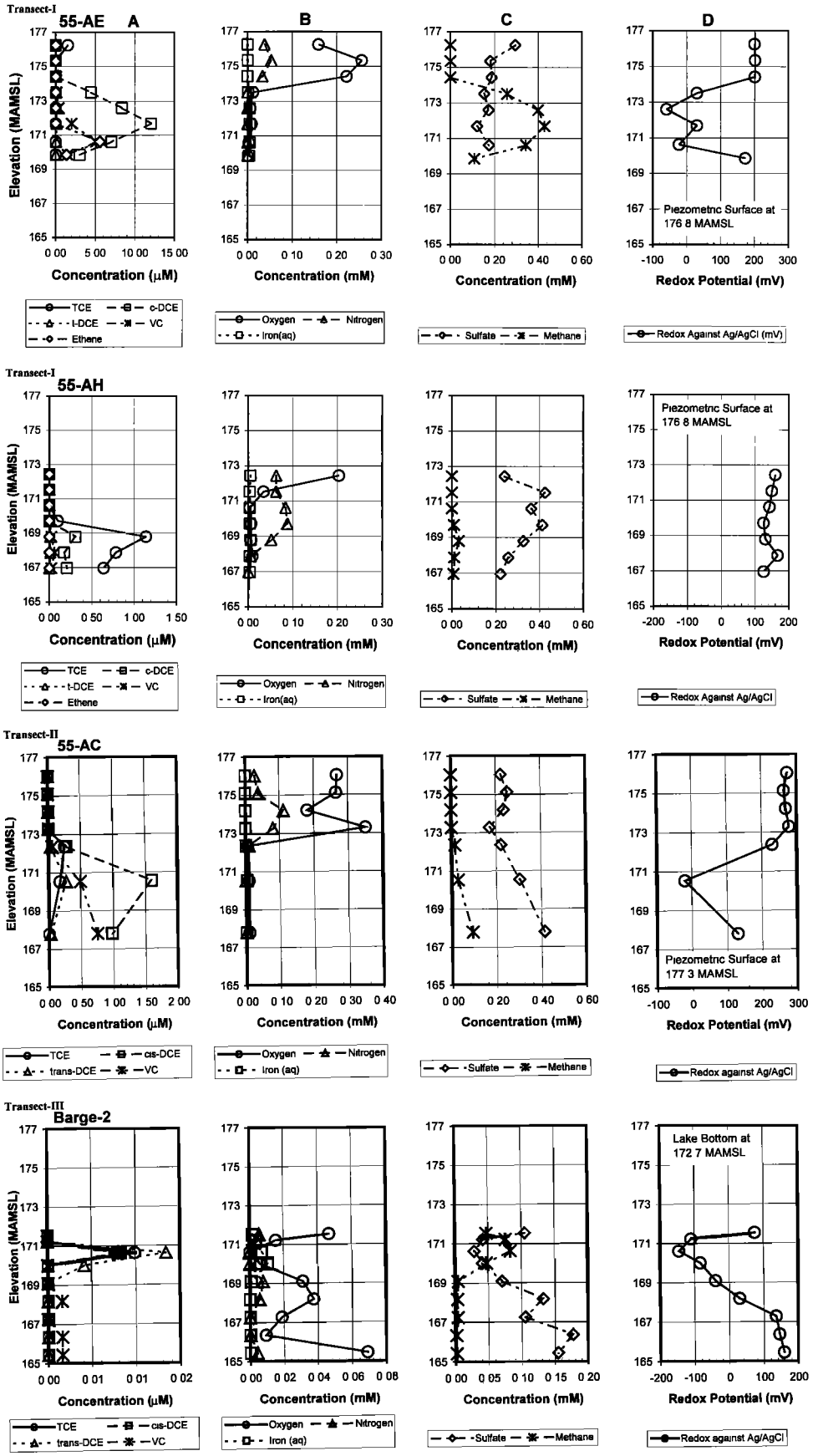

Figure 4. (a) Elevation profiles of contaminants, (b) redox-sensitive species of oxygen, total nitrogen, and total aqueous iron (II), (c) redox-sensitive species of sulfate and methane, and (d) redox potential for selected borings along transects I–III.

Table 1. Iron Speciation as a Function of Elevation in Selected Wells Along Transects I and II

Sample Point	Elevation, MAMSL	Dissolved Fe (II), mg L^{-1}	Bioavailable[a] Fe (III), mg kg^{-1} Aquifer Solids	Extractable[b] Fe (II), mg kg^{-1} Aquifer Solids
55-AE	175.3	0.05	58.0	215.5
55-AE	174.4	0.0	102.7	260.0
55-AE	173.5	0.1	28.8	207.3
55-AE	172.6	0.3	41.2	376.2
55-AE	169.8	0.2	4.9	697.6
55-AF	173.4	0.05	95.6	180.9
55-AF	172.4	0.0	30.2	209.9
55-AF	171.5	0.0	26.3	216.1
55-AF	170.6	0.2	59.42	614.0
55-AG	173.4	0.1	76.1	152.8
55-AG	172.4	0.1	62.8	177.1
55-AG	170.6	0.2	36.9	416.6
55-AG	169.7	0.1	36.5	810.6
55-AH	172.4	0.3	143.0	244.6
55-AH	170.6	0.2	142.1	482.6
55-AH	169.7	0.2	158.0	219.6
55-AH	168.8	0.3	115.5	193.8
55-AH	167.9	0.2	65.7	218.2
55-AH	167.0	0.2	79.7	288.7
55-AH	166.0	No Data	98.3	208.4
55-AI	172.7	0.2	38.2	230.2
55-AI	171.2	0.1	13.8	315.6

[a]As defined by *Lovley and Phillips* [1987].
[b]As defined by *Heron et al.* [1994] for a 1 hour extraction with 0.5 M HCl. Extractions were performed with wet aquifer solids and then corrected for the mass of water to yield iron concentrations as a function of dry solids.

negative to support sulfate reduction. No lake sediment extractions were performed to quantify solids-bound iron, but soluble iron was generally slightly higher when compared to transects I and II (Figure 4b).

A schematic representation of redox zonation at the GSI consistent with this analysis and discussion is presented in Figure 6. Considering the information from all transects, a gradual change in redox conditions at the GSI was apparent with distance from the shore and with depth. For example, between transects I and II the shallow sampling points became increasingly more oxidized and exhibited characteristics reflective of groundwater/surface water interactions (e.g., specific conductance and chloride). The deeper sampling points at transect I were more reduced, possibly sulfate-reducing to methanogenic as evidenced by elevated methane and reduced sulfate concentrations. This transect was closest to up-gradient transects, which were found to be predominantly sulfate-reducing to methanogenic, conditions conducive to extensive reductive dechlorination [*Semprini et al.*, 1995]. Up-gradient transects were mostly anaerobic and reduced, even at shallow sampling points. Low methane concentrations observed at beach transect II as well as elevated sulfate concentrations with elevation indicate reoxygenation of this transect by lake water infiltration relative to transect I. While the top 3 m of the aquifer were aerobic, geochemical profiles (Figure 4) and aquifer iron extraction data (Table 1 and Figure 5) of the deeper regions of the aquifer suggested denitrifying to iron-reducing conditions. As the groundwater flowed underneath the lake bottom, the redox conditions became more reducing (probably sulfate-reducing) on the basis of depleted sulfate concentrations and E_h measurements.

The delineation of redox conditions and zones of dominant TEAPs on the basis of platinum electrode measurements is limited predominantly by equilibrium assumptions and by the fact that E_h measurements reflect mixed potentials with little thermodynamic significance [*Lindbergh and Reynolds*, 1984; *Barcelona et al.*, 1989]. For example, redox species such as CO_2 and CH_4 exhibit poor electroreactivity [*Stumm and Morgan*, 1981], but iron species are highly electroactive, resulting in a bias in the predicted values based on the equilibrium stability diagrams. On the basis of literature reports, E_h measurements mainly permit a distinction between aerobic (measurable oxygen), reduced (no dissolved oxygen), and transitional (strong concentration gradients in principal oxidized or reduced species) zones [*Barcelona et al.*, 1989; *Barcelona and Holm*, 1991]. These and other studies [e.g., *Chapelle et al.*, 1996] point toward the need to supplement E_h measurements with redox

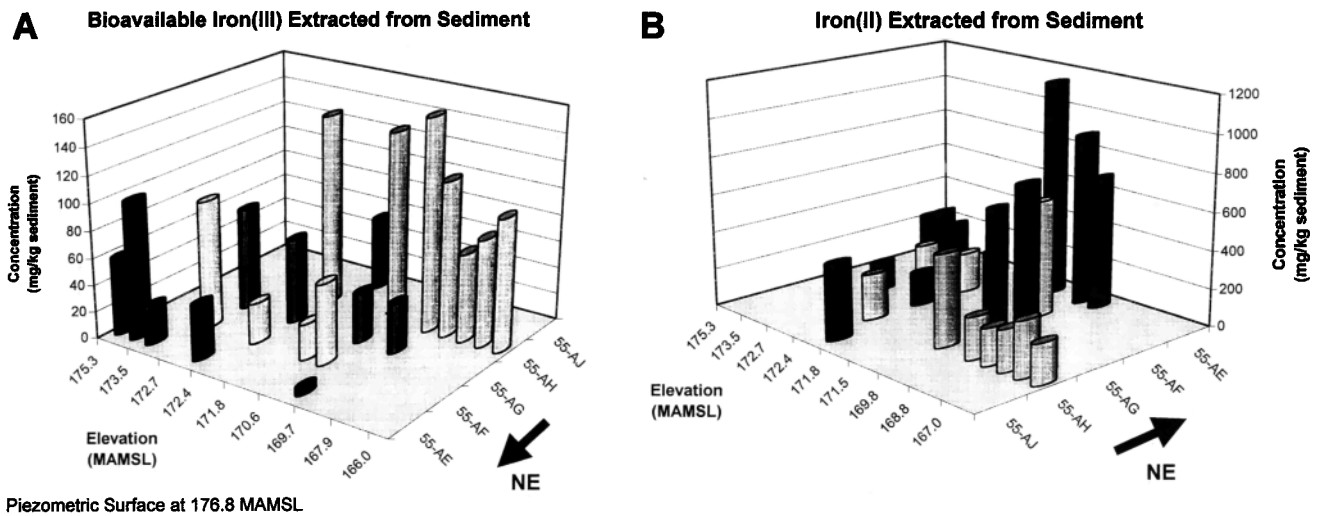

Figure 5. Aquifer solids-extracted iron concentrations along transect I as a function of elevation: (a) bioavailable iron (III) as defined by *Lovely and Philips* [1987] and (b) 0.5 M HCl acid extractable iron (II) as defined by *Heron et al.* [1994]. Note the display of sample locations is reversed between Figures 5a and 5b to allow for better visualization of trends.

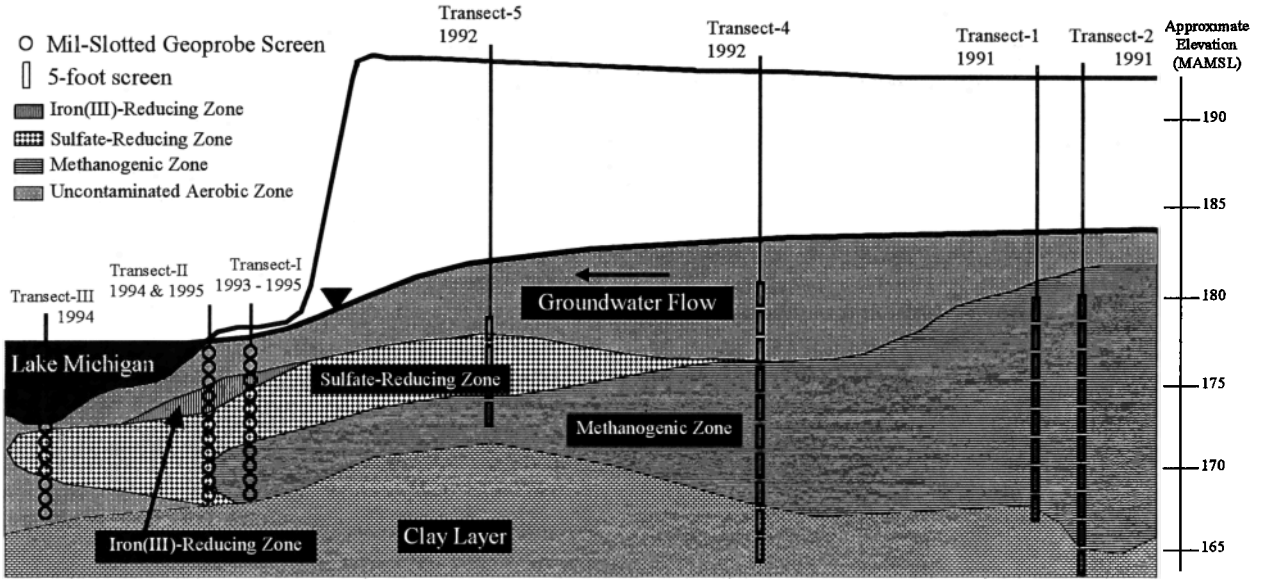

Figure 6. Proposed redox zonation along a longitudinal cross section of the groundwater/surface water interface (GSI).

pairs in groundwater or with other endpoints of microbial respiratory activity (such as dissolved hydrogen gas measurements). The latter requires the installation of permanent, nonelectrically conductive monitoring points to allow for stabilization of the aquifer solids perturbed after sampling point installation [*Lovley et al.*, 1994; *Chapelle et al.*, 1997].

The hydrology of groundwater/surface water interactions has demonstrated a positive correlation between the extent of wave infiltration and stability of shorelines [e.g., *Duncan*, 1964; *Devito et al.*, 1996]. On the basis of preliminary studies with a groundwater/surface water flow model constructed for this site, which included seiche activity and recorded wave heights during calm weather and storm events, an infiltration zone of influence was predicted to affect groundwater flow and reoxygenation within the top 2–3 m below the water table (176.5 MAMSL) [*Adriaens et al.*, 1997; *Dean*, 1998]. This correlated with the shallow sample locations observed in this study on the basis of chemical analyses.

4.3. Contaminant Distribution and Potential for Intrinsic Bioremediation

The spatial distribution of all contaminant concentrations with elevation is shown relative to groundwater elevation (~177 MAMSL) as a reference elevation for selected monitoring points at each transect in Figure 4a. Compared to concentrations in the source area, the contaminant concentrations were rather low (μM) at the beach transect and near the detection limit (0.003 μM) at the barge transect. These concentrations represent an exponential decrease relative to total CAH concentrations observed up-gradient which are in the mM range [*McCarty et al.*, 1991; *Semprini et al.*, 1995]. This observation would be consistent with dilution and dispersion effects along the contaminant flow line. Since inorganic chloride is a nonreactive tracer, a change in chloride concentration between transects may be indicative of dilution effects. Between the beach and barge transects, maximum chloride concentrations decrease (Figures 3a and 3b), which may in part be explained by a likely broad plume convergence zone between these sampling transects. This would result in significant dilution of the groundwater by lake water.

On the basis of the depth profiles observed for selected sample points in the beach transect, several trends were detected which differentiated these borings from those carried out up-gradient [*Semprini et al.*, 1995]. First, the shallow sample points consistently did not show any of the CAHs, except for sample point 55-AE which indicated 2 μM of TCE. It should be noted that these shallow zones were without exception aerobic and coincided with specific conductance and chloride concentrations similar to those of the surface water. The phenomenon of surface water infiltration in beach areas due to wave run-up and tidal events has been described extensively and was predicted recently for this site [*Adriaens et al.*, 1997]. It is thus conceivable that infiltration of aerobic surface water was not only responsible for the reoxygenation of the aquifer but also results in "erosion" of the plume. Second, the previously observed vertical stratification reported for up-gradient borings [*Semprini et al.*, 1995] was still apparent but was condensed over a narrower aquifer thickness. It should be noted that this observation was highly dependent on the location of the boring. Boring 55-AE, for example, exhibited maxima for TCE, *cis*-DCE, VC, and ethene at 176, 172, and 171 MAMSL, respectively (Figure 4a). The boring closer to the lake as part of transect II, 55-AC, showed maximum concentrations of the same CAH at slightly deeper locations: 172, 171, and 168 MAMSL, respectively. The contaminant concentrations of the boring on the fringe of the plume, 55-AH, are lower yet at elevations of 168–169 MAMSL. These elevations may be reflective of the extent of surface water infiltration and downward migration of the CAH as previously suggested [*Semprini et al.*, 1995]. Third, the contaminant concentrations increased in the NE direction by an order of magnitude, suggesting the longitudinal center line of the plume is either near 55-AE or to the NE.

Under reduced, predominantly methanogenic and sulfate-reducing conditions, chlorinated solvents can be expected to undergo reductive dechlorination reactions. Specifically, labo-

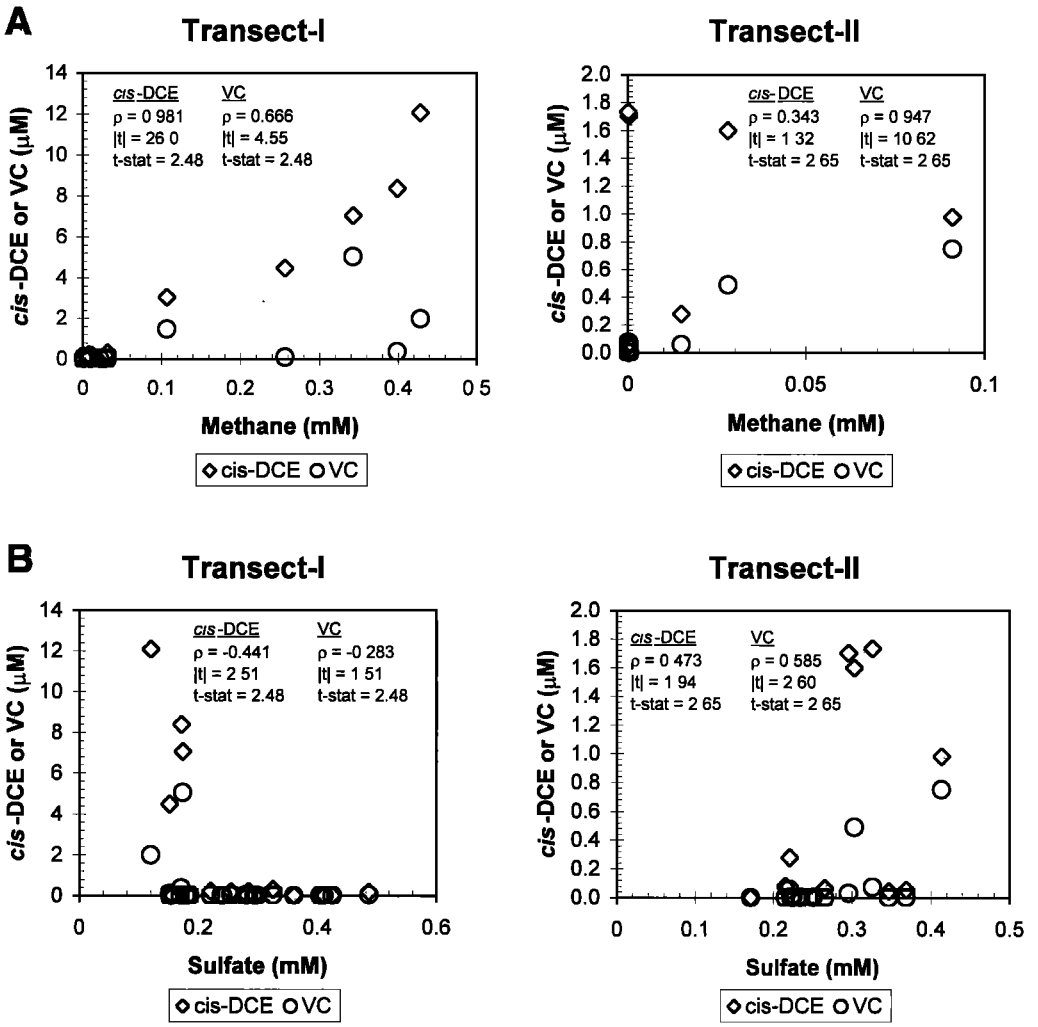

Figure 7. Scattergrams of (a) *cis*-DCE or VC with methane and (b) *cis*-DCE or VC with sulfate along transects I and II. Statistical analyses shown consist of correlation coefficient (ρ), $|t|$ based on a two-tailed t test, and the statistical determination of t (t-stat) using $\alpha = 0.01$ (99% confidence interval).

ratory and field demonstrations have shown that VC and ethene can be produced under methanogenic conditions [*Freedman and Gossett*, 1989; *DiStefano et al.*, 1991]; however, the DCE isomers have been found to be the endpoint under sulfate-reducing [*Haston et al.*, 1994; *Pavlostathis and Zhang*, 1991; *Bagley and Gossett*, 1990] and iron-reducing [*McCormick and Adriaens*, 1998] conditions. In the up-gradient regions, dechlorination was found to occur under both sulfate-reducing and methanogenic conditions in shallow and deep segments of the aquifer, respectively [*Semprini et al.*, 1995]. In an attempt to correlate product distribution with electron acceptor products, several trends were observed (Figures 4 and 6). At transect I, *cis*-DCE ($\rho = 0.981$) and VC ($\rho = 0.666$) exhibited significant correlations ($\alpha = 0.01$) with methane (Figure 7a); however, it should be noted that the correlation between *cis*-DCE and methane was stronger than that of VC and methane. At transect II, only VC ($\rho = 0.947$) exhibited a significant correlation ($\alpha = 0.01$) with methane (Figure 7a). No correlation ($\alpha = 0.01$) between *cis*-DCE or VC and depletion of sulfate was observed except for *cis*-DCE ($\rho = -0.441$) to sulfate at transect I. On an individual sample point basis both *cis*-DCE and VC were present in zones of methane production (55-AC and 55-AE) or sulfate depletion (55-AH); however, it should not be construed that these reductive dechlorination products are necessarily locally produced. Moreover, 55-AC and 55-AE also indicated elevated iron (II) concentrations (Figure 4b), and ethene was present in methanogenic regions of sample point 55-AE.

Since reductive dechlorination reactions require an organic or inorganic external electron donor the extent of dechlorination depends on the available electron equivalents for fortuitous reactions. Analyses of samples from sample points 55-AE through 55-AI along transects I and II indicated the presence of 1–15 mg L^{-1} of TOC which consisted, in part, of low molecular weight organic acids (e.g., benzoic, methylbenzoic, pentanoic, and hexanoic), corroborating results from up-gradient transects [*McCarty and Wilson*, 1992]. Aliphatic and aromatic acids were not analyzed in other beach and barge samples. As has been observed in many natural groundwaters, the identified organic acids in combination with contaminant concentrations do not account for the TOC results when summed, suggesting that other, possibly natural carbon sources, are available for microbial respiration. Since the St. Joseph aquifer is oligotrophic exhibiting very low fractions of organic carbon

Table 2. Calculated Maximum Contribution of Total Organic Carbon (TOC) in Electron Equivalents and Average Electron Equivalents Required for Chlorinated Aliphatic Hydrocarbon (CAH) Dechlorination to Ethene

Sample Point	Average TOC at Contaminated Sample Elevations, mg L^{-1}	e^- Equivalent Associated With TOC Mineralization,[a] μeq L^{-1}	e^- Equivalent Associated With TOC Hydroquinone-Quinone Redox,[b] μeq L^{-1}	e^- Equivalent Associated With CAH Dechlorination,[c] μeq L^{-1}
55-AE	13.9	4640	386	24.0
55-AF	2.05	683	57	7.63
55-AG	1.85	617	51	6.46
55-AH	2.08	692	58	4.76
55-AI	3.57	1190	99	0.62
Average	4.69	1570	130	8.69

[a]On the basis of the transfer of 4 electron equivalents during the mineralization of CH_2O to CO_2 and calculated using the equation e^- Equiv.(μeq L^{-1}) = [TOC(mg(C) L^{-1})/12 mg(C) mmol(C)$^{-1}$][4 meq/mmole(C)](1000 μeq/meq).
[b]On the basis of the transfer of 2 electron equivalents during the reduction of $C_6H_6O_2$ to $C_6H_4O_2$ and calculated using the equation e^- Equiv.(μeq L^{-1}) = [TOC(mg(C) L^{-1})/12 mg(C) mmol(C)$^{-1}$][mmol($C_6H_6O_2$)/6 mmol(C)][2 meq/mmol($C_6H_6O_2$)](1000 μeq/meq).
[c]Transfer of 2 electron equivalents for each reductive dechlorination step per mole of contaminant.

($0.02\% < f_{OC} < 0.07\%$) [*McCarty et al.*, 1991] the TOC may be derived from plant leachates and dissolved humic acids. These constituents can be represented by a hypothetical molecular formula of CH_2O [*Chapelle*, 1993; *Postma and Jakobsen*, 1996], if complete mineralization is considered, or of $C_6H_6O_2$ [*Barcelona and Holm*, 1991] in the case of quinone redox chemistry, as shown in (1) and (2), respectively.

$$CH_2O + H_2O \rightarrow CO_2 + 4H^+ + 4e^- \quad (1)$$

$$C_6H_6O_2 \rightarrow C_6H_4O_2 + 2H^+ + 2e^- \quad (2)$$

On the basis of this rationale the total moles of electrons (or electron equivalents) available from the mineralization of TOC to carbon dioxide or the quinone/hydroquinone redox couple may be compared to the electron equivalents required for reductive dechlorination of contaminants to ethene assuming two electrons are required for each dechlorination step (Table 2) [*Vogel et al.*, 1987]. On average the electron equivalents generated from the complete mineralization of TOC to carbon dioxide are 2 orders of magnitude higher than that required (per liter of groundwater) for complete dechlorination of CAHs to ethene. Even in the case of quinone reduction (one-twelfth the electron equivalents compared to mineralization of CH_2O) more than sufficient electron equivalents are also available for the dechlorination reactions. These data provide upper and lower bounds of electron equivalents available from the oxidation of TOC. While not all electron equivalents released in the oxidation processes could realistically be used to dechlorinate contaminants, these data indicate that TOC can provide a possible carbon source to microorganisms for fortuitous reductive dechlorination of CAHs at the GSI.

5. Conclusions

This study was aimed at evaluating the potential for natural processes affecting the disposition of chlorinated solvents at the groundwater/surface water interface (GSI) with a large lake and necessitated the implementation of several innovative monitoring techniques. Geophysical subsurface characterization methods such as GPR and sonar served to guide offshore sampling programs and helped to predict the likely locale of groundwater/surface water interactions. Despite the site heterogeneities which undoubtedly affected the interpretation of results from field-scale investigations, several geochemical trends and processes were identified: (1) the contaminant plume was transported and diluted in a relatively conductive subsurface layer which extended from the beach in an offshore direction; (2) wave run-up and lake water infiltration created a lakeward flux of contaminants in the near water table region ("plume erosion") and reoxygenated the top 3 m of the contaminant plume; (3) the deeper portion of the aquifer on the beach was not affected by lake water and remained highly reduced; (4) the offshore groundwater aquifer indicated sulfate reduction and did not show significant mixing with the aerobic lake water. Natural anaerobic dechlorination reactions have the greatest potential to occur in the deeper sulfate-reducing and methanogenic zones. Reoxygenation of the aquifer to hypoxic conditions may provide a suitable environment for aerobic commensalic or cometabolic biodegradation processes to occur. Considering the dynamic nature of this GSI, a continuing monitoring program needs to be implemented to adequately capture temporal changes in contaminant distribution and microbial biodegradative activity. Considering that methanogenic or sulfate-reducing conditions may not exist in transect II, the potential for either dechlorination [*McCormick and Adriaens*, 1998; *McCormick et al.*, 1998] or oxidation [*Bradley and Chapelle*, 1996] reactions under iron-reducing conditions deserves further attention.

Acknowledgments. Funding for this research was provided by EPA grant R-819605-01-4 awarded to PA, MJB, and WAS and via funding from the Research and Reeducation for Displaced Department of Defense Personnel (R2D2) program administered by the Great Lakes and Mid-Atlantic Hazardous Substance Research Center (GLMAC-HSRC) at the University of Michigan. Since these results have not been peer-reviewed by either agency, no endorsement should be inferred. The authors wish to acknowledge the support of F. Beck and M. Cook from the EPA National Risk Management Research Laboratory (Subsurface Protection and Remediation Division) for their assistance in obtaining field samples and chemical analysis of groundwater samples. G. Etzel of Bosch Breaking Systems is acknowledged for his support in obtaining access to the site and assistance in equipment repair. J. Brilliant is acknowledged for his assistance during aquifer solid extraction for bioavailable iron.

References

Adriaens, P., J. M. Lendvay, M. L. McCormick, and S. M. Dean, Biogeochemistry and dechlorination potential at the St. Joseph Aquifer-Lake Michigan interface, in *In Situ and On Site Bioremediation*, Vol. 3, edited by B. C. Alleman and A. Leeson, pp. 173–179, Batelle, Columbus, Ohio, 1997.

American Public Health Association, *Standard Methods for the Examination of Water and Wastewater*, 18th ed., Washington, D. C., 1992.

American Public Health Association, *Standard Methods for the Examination of Water and Wastewater*, 19th ed., Washington, D. C., 1995.

Bagley, D. M., and J. M. Gossett, Tetrachoroethene transformation to trichloroethene and cis-1,2-dichloroethene by sulfate-reducing enrichment cultures, *Appl. Environ. Microbiol.*, *56*, 2511–2516, 1990.

Barcelona, M. J., Geoprobe goes amphibious, *Probing Times*, *4*, 1, 1994.

Barcelona, M. J., and T. R. Holm, Oxidation-reduction capacities of aquifer solids, *Environ. Sci. Technol.*, *25*, 1565–1572, 1991.

Barcelona, M. J., T. R. Holm, M. R. Schock, and G. K. George, Spatial and temporal gradients in aquifer oxidation-reduction conditions, *Water Resour. Res.*, *25*, 991–1003, 1989.

Benson, A. K. Integrating ground penetrating radar and electrical resistivity data to delineate groundwater contamination, in *Fourth International Conference on Ground Penetrating Radar (GPR '92)*, edited by P. Hanninen and S. Autio, pp. 197–205, Geol. Surv. of Finland, Rovaniemi, Finland, 1992.

Bermejo, J. L., W. A. Sauck, and E. A. Atekwana, Geophysical discovery of a new LNAPL plume at the former Wurtsmoth AFB, Oscoda, MI, *Ground Water Monit. Remediation*, *17*, 131–137, 1997.

Bradley, P. M., and F. H. Chapelle, Anaerobic mineralization of vinyl chloride in Fe (III)-reducing aquifer sediments, *Environ. Sci. Technol.*, *30*, 2084–2086, 1996.

Campbell, D. L., J. C. Wynn, S. E. Box, A. A. Bookstrom, and R. J. Horton, Tests of ground penetrating radar and induced polarization for mapping of fluvial mine tailings on the floor of Coeur d'Alene river, Idaho, in *Proceedings of the Symposium on the Application of Geophysical Engineering to Environmental Problems (SAGEEP'97)*, edited by R. S. Bell, pp. 81–87, Environ. and Eng. Geophys. Soc., Englewood, Colo., 1997.

Chapelle, F. H., *Ground-Water Microbiology and Geochemistry*, John Wiley, New York, 1993.

Chapelle, F. H., S. K. Haack, P. Adriaens, M. A. Henry, and P. M. Bradley, Comparison of E_h and H_2 measurements for delineating redox processes in a contaminated aquifer, *Environ. Sci. Technol.*, *30*, 3565–3569, 1996.

Chapelle, F. H., D. A. Vroblesky, J. C. Woodward, and D. R. Lovley, Practical considerations for measureing hydrogen concentrations in groundwater, *Environ. Sci. Technol.*, *31*, 2873–2877, 1997.

Cherkauer, D. S., and J. McBride, A remotely operated seepage meter for use in large lakes and rivers, *Ground Water*, *30*, 165–171, 1988.

Cherkauer, D. S., and D. C. Nader, Distribution of groundwater seepage to large surface-water bodies: The effect of hydraulic heterogeneities, *J. Hydrol.*, *109*, 151–165, 1989.

Christensen, T. H., P. Kjeldsen, H. J. Albrechtsen, G. Heron, P. H. Nielsen, P. L. Bjerg, and P. E. Holm, Attenuation of landfill leachate pollutants in aquifers, *Crit. Rev. Environ. Sci. Technol.*, *24*, 119–202, 1994.

Cozzarelli, I. M., M. J. Baedecker, R. P. Eganhouse, and D. F. Goerlitz, The geochemical evolution of low-molecular weight organic acids derived from the degradation of petroleum hydrocarbon contaminants in groundwater, *Geochim. Cosmochim. Acta*, *58*, 863–877, 1994.

Curtis, G. P., and M. Reinhard, Reductive dehalogenation of hexachloroethane, carbon tetrachloride, and bromoform by anthrahydroquinone disulfonate and humic acid, *Environ. Sci. Technol.*, *28*, 2393–2401, 1994.

Daniels, J. J., Fundamentals of ground penetrating radar, in *Proceedings of the Symposium on the Application of Geophysical Engineering to Environmental Problems (SAGEEP'89)*, Environ. and Eng. Geophys. Soc., Englewood, Colo., 1989.

Dean, S. M., Effects of lake-ground water interactions on the transport and bioremediation of chlorinated solvents discharging to the Great Lakes, Ph.D. dissertation, Univ. of Mich., Ann Arbor, 1998.

Delaney, A. J., P. V. Sellmann, and S. A. Arcone, Sub-bottom profiling: A comparison of short-pulse radar and acoustic data, in *Fourth International Conference on Ground Penetrating Radar (GPR '92)*, edited by P. Hanninen and S. Autio, pp. 149–157, Geol. Surv. of Finland, Rovaniemi, Finland, 1992.

Devito, K. J., A. R. Hill, and N. Roulet, Groundwater-surface water interactions in headwater forested wetlands of the Canadian Shield, *J. Hydrol.*, *181*, 127–147, 1996.

DiStefano, T. D., J. M. Gossett, and S. H. Zinder, Reductive dechlorination of high concentrations of tetrachloroethene to ethene by anaerobic enrichment culture in the absence of methanogenesis, *Appl. Environ. Microbiol.*, *57*, 2287–2292, 1991.

Duncan, J. R., The effects of water table and tide cycle on swash-backlash sediment distribution and beach profile development, *Mar. Geol.*, *2*, 186–197, 1964.

Freedman, D. L., and J. M. Gossett, Biological reductive dechlorination of tetrachloroethylene and trichloroethylene to ethylene under methanogenic conditions, *Appl. Environ. Microbiol.*, *55*, 2144–2151, 1989.

Gibbs, C. R., Characterization and application of ferrozine iron reagent as a ferrous iron indicator, *Anal. Chem.*, *48*, 1197–1201, 1976.

Haston, Z. C., P. K. Sharma, J. N. P. Black, and P. L. McCarty, Enhanced reductive dechlorination of chlorinated ethenes, in *Symposium on Bioremediation of Hazardous Wastes: Research, Development, and Field Evaluations, Rep. EPA/600/R-94/075*, pp. 11–15, Environ. Prot. Agency, Washington, D. C., 1994.

Heron, G., and T. H. Christensen, Impact of sediment-bound iron on redox buffering in a landfill leachate polluted aquifer (Vejen, Denmark), *Environ. Sci. Technol.*, *29*, 187–192, 1995.

Heron, G., C. Crouzet, A. C. M. Bourg, and T. H. Christensen, Speciation of Fe(II) and Fe(III) in contaminated aquifer sediments using chemical extraction techniques, *Environ. Sci. Technol.*, *28*, 1698–1705, 1994.

Holliger, C., and W. Schumacher, Reductive dehcalogenation as a respiratory porcess, *Antonie van Leeuwenhoek*, *66*, 239–246, 1994.

Kampbell, D. H., J. T. Wilson, and S. A. Vandergrify, Dissolved oxygen and methane water by a GC headspace equilibration technique, *Int. J. Environ. Anal. Chem.*, *36*, 249–259, 1989.

Keck Consulting Services, Inc., Hydrology study: Final investigation, section 10, Lincoln Township, Berrien County, Mich., 1986.

King, T. V. V., and G. R. Olhoeft, Mapping organic contamination by detection of clay-organic processes, paper presented at Conference on Petroleum Hydrocarbons and Organic Chemicals in Ground Water: Prevention, Detection, and Restoration, *Natl. Groundwater Assoc., Westerville, Ohio, 1989.*

Kitanidis, P. K., L. Semprini, D. H. Kampbell, and J. T. Wilson, Natural anaerobic bioremediation of TCE at the St. Joseph, Michigan, superfund site, *Rep. EPA/600/R-93/126*, pp. 57–60, Environ. Prot. Agency, Washington, D. C., 1993.

Kriegman-King, M. R., and M. Reinhard, Transformation of carbon tetrachloride in the presence of sulfide, biotite, and vermiculite, *Environ. Sci. Technol.*, *26*, 2198–2206, 1992.

Lawton, D. C., H. M. Jol, and D. G. Smith, Ground penetrating radar surveys for near-surface characterization and contaminant mapping: Example from the Canada creosote site, Calgary, in *Abstracts of the Fifth International Conference on Ground Penetrating Radar (GPR '94)*, Waterloo Cent. for Groundwater Res., Waterloo, Ont., Canada, 1994.

Lee, D. R., A device for measuring seepage flux in lakes and estuaries, *Limnol. Oceanogr.*, *22*, 140–147, 1977.

Lendvay, J., M. McCormick, and P. Adriaens, Intrinsic bioremediation of trichloroethylene at the St. Joseph Aquifer/Lake Michigan interface: A role for iron and sulfate reduction, in *Symposium on Bioremedial Hazardous Wastes: Research, Development and Field Evaluations*, pp. 3–6, *Rep. EPA/600/R-95/076*, Environ. Prot. Agency, Washington, D. C., 1995.

Lindberg, R. D., and D. D. Reynolds, Groundwater redox reactions: An analysis of equilibrium state applied to E_h measurements and geochemical modeling, *Science*, *225*, 925–927, 1984.

Lovley, D. R., and F. H. Chapelle, Deep subsurface microbial processes, *Rev. Geophys.*, *33*, 365–381, 1995.

Lovley, D. R., and S. Goodwin, Hydrogen concentrations as an indicator of the predominant terminal electron-accepting reactions in aquatic sediments, *Geochim. Cosmochim. Acta*, *52*, 2993–3003, 1988.

Lovley, D. R., and E. J. P. Phillips, Competitive mechanisms for inhibition of sulfate-reduction and methane production in the zone of ferric iron(III) reduction in sediments, *Appl. Environ. Microbiol.*, *53*, 2636–2641, 1987.

Lovley, D. R., F. H. Chapelle, and J. C. Woodward, Use of dissolved H_2 concentrations to determine distribution of microbially catalyzed redox reactions in anoxic groundwater, *Environ. Sci. Technol.*, *28*, 1205–1210, 1994.

Maxwell, M., and J. Schmok, Detection and mapping of an LNAPL plume using GPR: A case study, in *Proceedings of the Symposium on the Application of Geophysics to Engineering and Environmental Prob-*

lems (*SAGEEP '95*), Environ. and Eng. Geophys. Soc., Englewood, Colo., 1995.

McBride, M. S., and K. O. Pfannkuch, The distribution of seepage within lakebeds, *J. Res. U.S. Geol. Surv.*, *3*, 505–572, 1975.

McCarty, P. L., and J. T. Wilson, Natural anaerobic treatment of a TCE plume St. Joseph, Michigan, NPL site, *Rep. EPA/600/R-92/126*, pp. 47–50, Environ. Prot. Agency, Washington, D. C., 1992.

McCarty, P. L., L. Semprini, M. E. Dolan, T. C. Harmon, C. Tiedeman, and S. M. Gorelick, In situ methanotrophic bioremediation for contaminated groundwater at St. Joseph, Michigan, in *On-Site Bioreclamation*, edited by R. E. Hinchee and R. F. Olfenbuttel, pp. 16–40, Butterworth-Heinemann, Newton, Mass., 1991.

McCormick, M. L., H. S. Kim, P. Adriaens, and E. J. Bouwer, Abiotic transformation of chlorinated solvents as a consequence of microbial iron reduction: An investigation of the role of biogenic magnetite in mediating reductive dechlorination, in *Proceedings of the 30th Mid-Atlantic Industrial and Hazardous Waste Conference*, Technomic, Lancaster, Penn., 1998.

McMahon, P. B., and F. H. Chapelle, Microbial production of organic acids in aquitard sediments and its role in aquifer geochemistry, *Nature*, *349*, 233–235, 1991.

Monier-Williams, M., Properties of light non-aqueous phase liquids and detection using commonly applied shallow sensing geophysical techniques, in *Proceedings of the Symposium on the Application of Geophysics to Engineering and Environmental Problems* (*SAGEEP '95*), Environ. and Eng. Geophys. Soc., Englewood, Colo., 1995.

Nash, M. S., E. Atekwana, and W. A. Sauck, Geophysical investigation of anomalous conductivity at a hydrocarbon contaminated site, in *Proceedings of the Symposium on the Application of Geophysics to Engineering and Environmental Problems* (*SAGEEP'97*), Environ. and Eng. Geophys. Soc., Englewood, Colo., 1997.

Olhoeft, G. R., J. E. Lucius, and R. M. Bochicchio, Scales of length and connectivity from ground penetrating radar, in *U.S. Geological Survey Toxic Substances Hydrology Program: Proceedings of the Technical Meeting, Phoenix, AZ*, edited by G. E. Mallard and S. E. Ragone, *U.S. Geol. Surv. Water Resour. Invest. Rep.*, *88-4220*, 1988.

Pavlostathis, S. G., and P. Zhuang, Transformation of trichloroethylene by sulfate-reducing cultures enriched from a contaminated soil, *Appl. Microbiol. Biotechnol.*, *36*, 416–420, 1991.

Pavlostathis, S. G., and P. Zhuang, Reductive dechlorination of chloroalkenes in microcosms developed with a field contaminated soil, *Chemosphere*, *27*, 585–595, 1993.

Postma, D., and R. Jakobsen, Redox zonation: Equilibrium constraints on the Fe(III)/SO_4^{2-} reduction interface, *Geochim. Cosmochim. Acta*, *60*, 3169–3175, 1996.

Rifai, H. S., R. C. Borden, J. T. Wilson, and C. H. Ward, Intrinsic bioattenuation for subsurface restoration, in *Intrinsic Bioremediation*, edited by R. E. Hinchee, J. T. Wilson, and D. C. Downey, pp. 1–31, Batelle, Columbus, Ohio, 1995.

Sacks, L. A., J. S. Herman, L. F. Konikow, and A. L. Vela, Seasonal dynamics of groundwater-lake interactions at Doñana National Park, Spain, *J. Hydrol.*, *136*, 123–154, 1992.

Sauck, W. A., and J. McNeil, Some problems associated with GPR detection of hydrocarbon plumes, in *Abstracts of the Fifth International Conference on Ground Penetrating Radar* (*GPR'94*), Waterloo Cent. for Groundwater, Waterloo, Ont., Canada, 1994.

Sauck, W. A., E. A. Atekwana, and M. S. Nash, High conductivities associated with an LNAPL plume imaged by integrated geophysical techniques, *J. Environ. Eng. Geophys.*, *2*, 203–212, 1997.

Semprini, L., P. K. Kitanidis, D. H. Kampbell, and J. T. Wilson, Anaerobic transformation of chlorinated aliphatic hydrocarbons in a sand aquifer based on spatial chemical distributions, *Water Resour. Res.*, *31*, 1051–1062, 1995.

Shedlock, R. J., D. A. Wilcox, T. A. Thompson, and D. A. Cohen, Interactions between ground water and wetlands, southern shore of Lake Michigan, USA, *J. Hydrol.*, *141*, 127–155, 1993.

Simpkins, W. W., and T. B. Parkin, Hydrogeology and redox geochemistry of methane in a late Wisconsonian till and loess sequence in central Iowa, *Water Resour. Res.*, *29*, 3643–3657, 1993.

Stookey, L. L., FerroZine: A new spectrophotometric reagent for iron, *Anal. Chem.*, *42*, 779–781, 1970.

Strobel, M. L., Assessment of information on ground-water/surface-water interactions in the northern midcontinent, paper presented at First International Conference on Water Resources Engineering, Am. Soc. of Civ. Eng., San Antonio, Tex., 1995.

Stumm, W., and J. J. Morgan, Aquatic Chemistry, *An Introduction Emphasizing Chemical Equilibria in Natural Waters*, 2nd ed., John Wiley, New York, 1981.

Tiedeman, C., and S. M. Gorelick, Analysis of Uncertainty in Optimal Groundwater Contaminant Capture Design, *Water Resour. Res.*, *29*, 2139–2153, 1993.

U.S. Environmental Protection Agency (EPA), Chloride in water-Titrimetric-Storet No. 00940 in EPA Methods for Chemical Analysis of Water and Wastes, *Rep. EPA/600/4-79-020*, Washington, D. C., 1979.

U.S. Environmental Protection Agency (EPA), Test methods for evaluating solid waste, *Rep. SW-846*, 3rd ed., Washington, D. C., 1986.

Vanek, V., Groundwater regime of a tidally influenced coastal pond, *J. Hydrol.*, *151*, 317–342, 1993.

Vogel, T. M., C. S. Criddle, and P. L. McCarty, Transformation of halogenated aliphatic compounds, *Environ. Sci. Technol.*, *21*, 722–736, 1987.

Wackett, L. P., Bacterial cometabolism of halogenated organic compounds, in *Microbial Transformation and Degradation of Toxic Organic Chemicals*, edited by L. Y. Young and C. E. Cerniglia, pp. 217–243, Wiley-Liss, New York, 1995.

Wersin, P., P. Hohener, R. Giovanoli, and W. Stumm, Early diagenetic influences on iron transformations in a freshwater lake sediment, *Chem. Geol.*, *90*, 233–252, 1991.

Wilson, J. T., J. W. Weaver, and D. H. Kampbell, Intrinsic Bioremediation of TCE in Ground Water at an NPL Site in St. Joseph, Michigan, in *Symposium on Intrinsic Bioremediation of Ground Water*, *Rep. EPA/540/R-94/515*, pp. 154–160, Washington, D. C., 1994.

P. Adriaens, M. J. Barcelona, J. M. Lendvay, and M. L. McCormick, Environmental and Water Resources Engineering, Department of Civil and Environmental Engineering, University of Michigan, Ann Arbor, MI 48109-2125. (e-mail: adriaens@engin.umich.edu)

D. H. Kampbell and J. T. Wilson, Subsurface Protection and Remediation Division, U.S. Environmental Protection Agency, 919 Kerr Research Drive, Ada, OK 74820.

W. A. Sauck, Department of Geology, Institute for Water Sciences, Western Michigan University, Kalamazoo, MI 49008-5150.

(Received April 3, 1998; revised May 7, 1998;
accepted May 18, 1998.)